

An ice-core proxy for Antarctic circumpolar zonal wind intensity

Yuping YAN,^{1,2} Paul A. MAYEWSKI,^{1,3} Shichang KANG,^{1,4} Eric MEYERSON^{1,3}

¹Climate Change Institute, University of Maine, 303 Bryand Global Sciences Center, Orono, ME 04469-5790, USA
E-mail: yyan@maine.edu

²National Climate Center, China Meteorological Administration, 46 Zhongguancun Nandajie, Haidian District, Beijing 10081, China

³Department of Earth Sciences, 5790 Bryand Global Sciences Center, University of Maine, Orono, ME 04469-5790, USA

⁴Institute of Tibetan Plateau Research, Chinese Academy of Sciences, 18 Shuangqing Road, Haidian District, Beijing 100085, China

ABSTRACT. Using US National Centers for Environmental Prediction/US National Center for Atmospheric Research re-analysis data, we investigate the relationships between crustal ion (nssCa²⁺) concentrations from three West Antarctic ice cores, namely, Siple Dome (SD), ITASE00-1 (IT001) and ITASE01-5 (IT015), and primary components of the climate system, namely, air pressure/geopotential height, zonal (*u*) and meridional (*v*) wind strength. Linear correlation analyses between nssCa²⁺ concentrations and both air-pressure and wind fields for the period of overlap between records indicate that the SD nssCa²⁺ variation is positively correlated with spring circumpolar zonal wind, while IT001 nssCa²⁺ has a positive correlation with circumpolar zonal wind throughout the year ($r > 0.3$, $p < 0.01$). Intensified Southern Westerlies circulation is conducive to transport of more crustal aerosols to both sites. Further correlation analyses between nssCa²⁺ concentrations from SD and IT001 and atmospheric circulation suggest that the high inland plateau (represented by core IT001) is largely influenced by transport from the upper troposphere. IT015 nssCa²⁺ is negatively correlated with westerly wind in October and November, suggesting that stronger westerly circulation may weaken the transport of crustal species to IT015. Correlations of nssCa²⁺ from the three ice cores with the Antarctic Oscillation index are consistent with results developed from the wind-field investigation. In addition, calibration between nssCa²⁺ concentration and the multivariate El Niño–Southern Oscillation (ENSO) index shows that crustal species transport to IT001 is enhanced during strong ENSO events.

1. INTRODUCTION

Ice-core records provide proxy information on local climate (accumulation and temperature via isotopes of water), regional climate (atmospheric circulation via wind-blown dust and sea salt), climate over hemispheric to global scales (trapped-gas records of carbon dioxide, methane, nitrous oxide and other gases), and conditions beyond the Earth (concentrations of extraterrestrial dust and cosmogenic isotopes). The chemical composition of polar snow and ice reflects the characteristics of the atmospheric pathway transporting the chemistry (e.g. Mayewski and others, 1997), changes in source emission strength, and post-depositional effects for reversible species (not utilized in this study; e.g. Legrand and Mayewski, 1997; Wolff and others, 2003).

Instrumental climate records are relatively sparse over the Southern Hemisphere and extend back typically <50 years. Glaciochemical proxy data can extend the paleoclimate record back hundreds to thousands of years and also provide a unique resource for examining changes in the sources, pathways and distribution of chemical species in the atmosphere through time (Mayewski and others, 1993).

The sources of chemical species deposited in polar snow and ice have been summarized in numerous papers (e.g. Herron, 1982; Lyons and Mayewski, 1984; Steffensen, 1988; Delmas and Legrand, 1989; Shaw, 1989; Davidson and others, 1992; Mayewski and others, 1992; Whitlow and others, 1994; Legrand and Mayewski, 1997; Röthlisberger and others, 2002). Calcium in polar snow has two major sources: sea-salt (ss) and crustally derived non-sea-salt (nss)

aerosols (Mayewski, and others, 1997). Increases in crustal source species indicate enhanced atmospheric turbidity, increased aridity in the source area and/or increased exposure of ice-free areas (Mayewski and Lyons, 1982; Mumford and Peel, 1982). Previous studies suggest that aerosol transport is highly correlated with sea-level pressure (SLP) in Antarctica, Greenland and Asia (Kreutz and others, 1997, 2000; Mayewski and others, 1997; Fischer, 2001; Kang and others, 2002, 2003; Meeker and Mayewski, 2002; Souney and others, 2002). This paper focuses on the non sea-salt calcium ($\text{nssCa}^{2+} = \text{Ca}^{2+} - (0.038 \times \text{Na}^+)$) time series from the three ice cores from West Antarctica and investigates the relationships between nssCa²⁺ and atmospheric circulation using US National Centers for Environmental Prediction (NCEP)/US National Center for Atmospheric Research (NCAR) re-analysis meteorological data.

2. DATA

Ice cores recovered from West Antarctica by the United States component of the International Trans-Antarctic Scientific Expedition (US ITASE) and during the Siple Dome project (ITASE 00-1 (IT001), ITASE 01-5 (IT015) and Siple Dome (SD)) were selected for this study (Fig. 1; Table 1). The SD core glaciochemistry was previously reported (Mayewski and others, 1995; Kreutz and others, 1996, 1999, 2000) and annually dated by Kreutz and others (1999). The other two cores were drilled during the US ITASE West Antarctic traverses of 1999–2001 and analyzed at sub-annual, continuous resolution (Kaspari and others, 2004; Dixon and

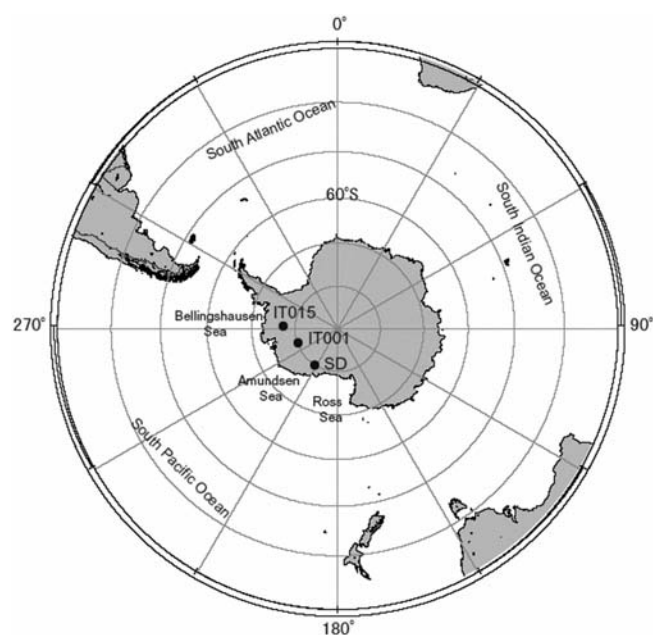


Fig. 1. Location map for the three core sites in West Antarctica.

others, 2005). The ITASE cores were processed at an average resolution of ~ 50 samples m^{-1} . Samples were examined for their major soluble ions (Na^+ , K^+ , Mg^{2+} , Ca^{2+} , Cl^- , NO_3^- , SO_4^{2-}) using a DX-500 ion chromatograph (IC) coupled to a Gilson[®] autosampler. Major cations (Na^+ , Ca^{2+} , Mg^{2+} and K^+) were determined using a CS-12a column with 25 Mm methanesulfonate (MSA) eluent. Antarctic samples may contain dissolved ions at very low concentrations. Detection limits, analytical variability and blank measurements are important for establishing confidence in reporting low values. Based on several tests of multiple runs, the IC detection limits for Na^+ and Ca^{2+} are 0.1 ppb, with analytical variability of 0.17 ppb for Na^+ and 0.22 ppb for Ca^{2+} . Blank concentrations are 0 ppb. Also crucial to achieving low detection limits are ice-handling techniques. During collection, core sections are minimally handled, and personnel wear plastic gloves and face masks. Core processing is performed using a continuous melting system which minimizes exposure of the samples to contamination. Further, IC analysis does not require the addition of reagents or dilution with water.

Cores are annually dated by matching seasonal peaks from each of the ion time series (Dixon and others, 2005). A 'core-chemistry' year is defined by a winter–spring peak in Na^+ , K^+ , Mg^{2+} , Ca^{2+} and Cl^- combined with spring–summer peaks in both NO_3^- and $xsSO_4^{2-}$ in accord with the seasonal timing

identified by previous research (e.g. Whitlow and others, 1994; Wagenbach, 1996; Legrand and Mayewski, 1997; Kreutz and Mayewski, 1999; Sommer and others, 2000).

Mean concentrations of major ions in the three ice cores are shown in Table 2. Na^+ and Cl^- concentrations are an order of magnitude higher than K^+ , Mg^{2+} and Ca^{2+} values, indicating the strong marine impacts on the region. Iterative testing of potential conservative sea-salt species following techniques described by O'Brien and others (1995) shows that Na^+ is a conservative indicator of sea salt and that, as a consequence, most of the Ca^{2+} in IT001 and IT015 (87% and 83.3%, respectively) is of crustal origin.

Numerical analyses involving European Centre for Medium-Range Weather Forecasts (ECMWF) datasets have played an important role in a variety of atmospheric studies in the high southern latitudes (e.g. Trenberth and Solomon, 1994; Bromwich and others, 1995, 2000; Budd and others, 1995; Cullather and others, 1996; Reijmer and others, 2002). ECMWF analyses are generally found to offer a reasonable depiction of broad-ranging atmospheric circulation, pressure-level fields and surface winds when compared to Antarctic automatic weather station (AWS) and ship observations (Cullather and others, 1997). However, a major obstacle to using operationally analyzed data for climate studies is the effect of alterations in the data assimilation system on the climatic ensemble of analyses (Trenberth, 1992). An alternative is to use NCEP/NCAR re-analysis data (Trenberth, 1995; Kalnay and others, 1996; Simmonds and Keay, 2000). The NCEP/NCAR analyses were obtained by assimilating past data into a frozen state-of-the-art analysis/forecast model system. The database was enhanced with many sources of observations that were not available in real-time operations, and the product is regarded as one of the most complete, physically consistent meteorological datasets (Simmonds and Keay, 2000). The NCEP/NCAR re-analysis archive is provided by the National Oceanic and Atmospheric Administration–Cooperative Institute for Research in Atmospheric Sciences (NOAA–CIRES) Climate Diagnostics Center, Boulder, CO, USA (<http://www.cdc.noaa.gov>). It contains monthly averaged analyses (reported every 6 hours from 0000 UTC) on a 2.5° latitude–longitude grid, at 17 standard pressure levels, as well as surface- and boundary-level variables for the period 1948–2002.

The Antarctic Oscillation (AAO) is the dominant pattern of non-seasonal tropospheric circulation variations south of $20^\circ S$, and is characterized by pressure anomalies of one sign centered in the Antarctic, and of the opposite sign centered close to 40 – $50^\circ S$. The AAO is also referred to as the Southern Annular Mode. It is defined as the leading principal component of the 850 hPa geopotential height anomalies south of $20^\circ S$ (Thompson and Wallace, 2000).

Table 1. Ice cores in West Antarctica

Site	Location	Elevation m a.s.l.	Depth m	Time period years AD	Sampling resolution cm	Full record period	
						Mean w.e. $cm a^{-1}$	Std dev.
Siple Dome-94	81.65° S, 149.0° W	620	150	1890–1995	2–25	11.8	22.0
ITASE 00-1	79.38° S, 111.24° W	1791	105	1653–2002	1.5–3.5	38.8	10.19
ITASE 01-5	77.06° S, 89.14° W	1246	114	1780–2001	1.6–3.5	4.67	4.32

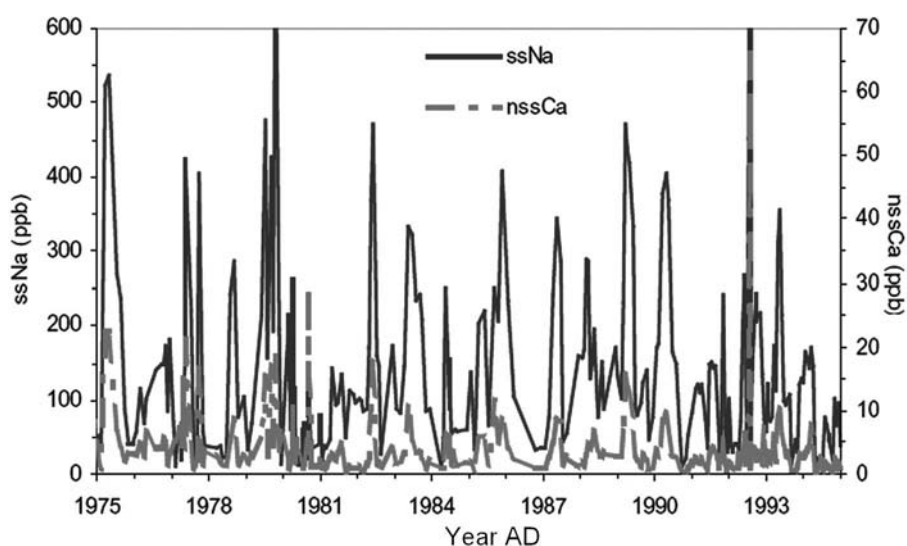


Fig. 2. A recent 20 year section of seasonal variations of sea-salt aerosol (ssNa^+) and nssCa^{2+} concentrations at SD.

To investigate potential associations between crustal species concentrations and atmospheric circulation, we use the available NCEP/NCAR instrumented/ modeled meteorological data, namely, zonal (u) and meridional (v) wind, and geopotential height, as well as AAO to compare with nssCa^{2+} from three ice cores.

3. RESULTS AND DISCUSSION

3.1. Relationships between SD nssCa^{2+} and atmospheric circulation, 1948–95

The input timing of marine aerosols (ssNa^+) to SD is from September to November (SON; Kreutz and others, 2000). Comparison of nssCa^{2+} with ssNa^+ concentrations at SD over the last 1000 years indicates the same inputting time for the two species. Seasonal variations of the two species over the last 20 years are shown in Figure 2, and indicate similar trends. The long-term (1948–95) seasonal mean of the 850 hPa zonal wind field is characterized by circumpolar westerly circulation (Fig. 3a). Stronger zonal winds ($>12 \text{ m s}^{-1}$) occur over the southeast and southwest sectors of the Indian Ocean. The positive correlation between seasonal (SON) mean 850 hPa zonal wind and SD nssCa^{2+} concentration (Fig. 3b) is significant (at the 95% confidence level) in the belt of westerly circulation, suggesting that strong westerly winds are conducive to transport of crustal aerosols to SD. Correlation analyses at higher levels in the atmosphere (500 hPa) reveal a similar region of westerly wind influence (Fig. 3c). Significantly correlated regions reduce in size or disappear at this level, even though wind speeds increase by $6\text{--}10 \text{ m s}^{-1}$ (Fig. 3c

and d), indicating that the transport of crustal aerosols to SD is mostly influenced by the lower-tropospheric circulation. Carleton (1989) notes that the belt of westerlies in the high-latitude Southern Hemisphere includes traveling wave cyclones, which originate in the lower middle latitudes, move poleward and intensify and stagnate along the coast of Antarctica in four general locations (Amundsen Sea, Weddell Sea, southeast and southwest Indian Ocean). These wave cyclones could carry not only heat and moisture poleward (Rogers, 1983), but also crustal dust at the same time.

The zonal anomalies of seasonal mean geopotential height at 500 hPa in SON (Fig. 4a) are characterized by a sharp gradient (60–150 m geopotential height) in the South Pacific and the southeast and southwest of the Indian Ocean in the $45\text{--}65^\circ \text{ S}$ region (gradients are smaller at lower levels). The western ridge of increased geopotential height creates a west-to-east pressure gradient that intensifies winds over the southwest and southern sectors of the Indian Ocean (Fig. 4b). These winds could deliver crustal aerosols from South America and South Africa to the West Antarctic atmosphere as demonstrated by difference fields for the seasonal u component in SON at 500 hPa (Fig. 4b). Westerly flow decreases (by $4\text{--}6 \text{ m s}^{-1}$) in the South Pacific $45\text{--}60^\circ \text{ S}$ region and increases (by $4\text{--}6 \text{ m s}^{-1}$) at the same latitude in the south Indian Ocean, as well as in the Ross Sea region (zonal wind velocity differences at lower levels are smaller). Crustal aerosols are spiraled into West Antarctica by these strong westerly winds. Comparison of the differences in zonal wind patterns with the correlation patterns (Fig. 3b and d) verifies the similarity.

Table 2. Summary of ion chemistry: average concentrations (ppb) for the overlap period. Values in parentheses are % of non-sea-salt calcium relative to total calcium

	Na^+	K^+	Mg^{2+}	Ca^{2+}	Cl^-	NO_3^-	SO_4^{2-}	nssCa^{2+}
SipleDome-94	154.0	7.2	23.2	8.2	299.2	35.0	114.7	2.4 (29.3)
ITASE00-1	28.0	2.6	3.6	6.9	46.1	36.6	38.1	6.0 (87.0)
ITASE01-5	30.3	2.8	4.6	6.0	53.5	31.9	36.6	5.0 (83.3)

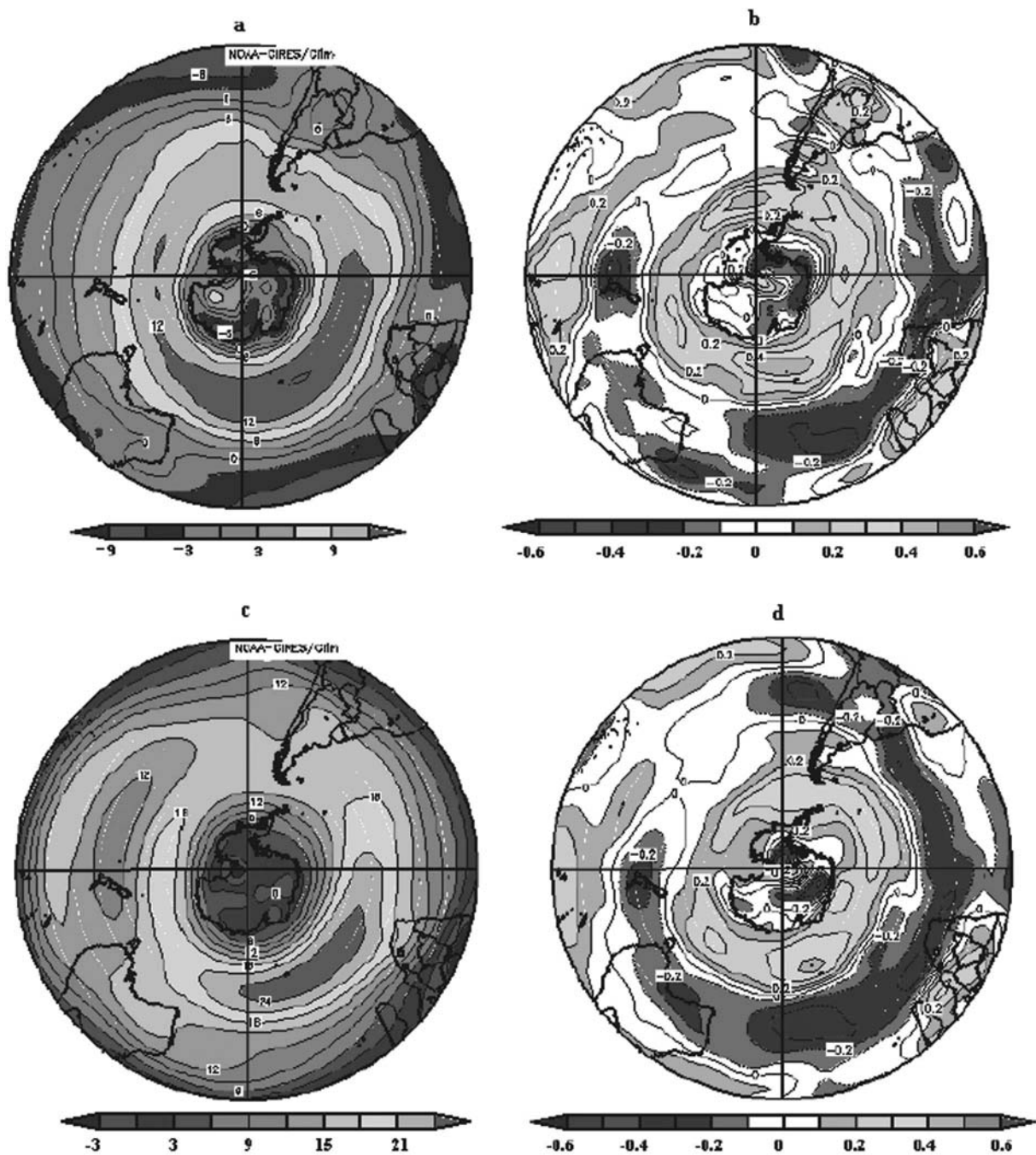


Fig. 3. (a, b) Seasonal mean 850 hPa zonal wind (a) and its spatial correlation patterns with SD nssCa²⁺ (b), for the period 1948–95, plotted as correlation coefficients. (c, d) Same as (a) and (b) respectively, but for 500 hPa zonal wind.

There is also a large region of low geopotential height around the Ross Sea (Fig. 4a), consistent with the strong westerly winds in this area (Fig. 4b). The Ross Sea area is the average center of the circumpolar vortex. Crustal aerosol is transported from the coast to the vicinity of SD under the influence of cyclonic storms in the Ross Sea.

The foregoing suggests that lower-tropospheric transport is more important than that at higher levels and the region of maximum zonal wind is around 60° S. Simmonds and Key (2000) noted that the axis of maximum Southern Hemisphere (SH) cyclogenesis lies at, or to the south of, 60° S. The lower-level (850 hPa) seasonal zonal mean wind at 60° S during SON is significantly correlated with nssCa²⁺ concentration at SD ($r = 0.38$, $p < 0.005$; $r = 0.33$, $p < 0.01$ for the period since 1968; Fig. 5a). From 1958 to 1967, however,

the 850 hPa seasonal zonal mean wind at 60° S has a weakly negative correlation with SD nssCa²⁺ concentration, a correlation that does not occur at 500 hPa atmosphere. The reason for this needs further work. It may be that the atmospheric boundary layer is easily affected by local climate when the circumpolar vortex is weak. In- and out-of-phase relationships between climate variables have been identified in previous Antarctic climate studies (e.g. Cul-lather and others, 1996).

SON seasonal mean meridional wind velocities are much smaller than zonal wind velocities and there is no apparent correlation between nssCa²⁺ and meridional wind. Also the correlation pattern is irregular. Therefore, the correlation between meridional circulation and nssCa²⁺ at SD is not significant.

Further analysis shows that nssCa^{2+} from SD is also correlated with monthly AAO (June–October; average $r = 0.34$, $p < 0.01$ for the period 1948–95), with the most significant correlations occurring in July ($r = 0.43$, $p < 0.005$) (Fig. 5b). This result is consistent with Harris' (1992) work, which indicates that the most vigorous long-range transport to the South Pole occurs from July through October.

3.2. Relationships between IT001 nssCa^{2+} and atmospheric circulation, 1948–2002

Generally the IT001 is little affected by the marine boundary atmosphere due to its high elevation (Tables 1 and 2). Most of the IT001 Ca^{2+} originates from continental source dust (about 87%; Table 2). There is no obvious seasonal variation for nssCa^{2+} concentration at IT001. It is positively correlated with zonal wind in circumpolar areas throughout the year, especially at higher atmospheric levels (e.g. mid- and upper troposphere), suggesting that the nssCa^{2+} in IT001 is transported through the mid- and upper troposphere ($r > 0.3$, $p < 0.01$). The influence of westerly circulation on the circumpolar areas is apparent throughout the year (only July is shown in Fig. 6). IT001 nssCa^{2+} has the highest mean concentration (6.0 ppb) of the three ice cores. The elevation of IT001 is ~ 1171 m higher than that of SD, and the nssCa^{2+} is probably transported over long distances by westerly circulation in the mid- to upper troposphere throughout the year.

Since upper-tropospheric westerly circulation is significantly correlated with the nssCa^{2+} at IT001, we compare the annually averaged 500 hPa zonal mean wind at 60°S with nssCa^{2+} concentrations. In general, variations in nssCa^{2+} are consistent with zonal mean wind at 60°S ($r = 0.44$, $p < 0.001$; Fig. 7a). Investigation of the relationship between nssCa^{2+} concentration and AAO indicates a significant positive correlation between the two time series for most of the year, except January when westerly flow is weakest and wind speed is lowest. The average correlation coefficient for 11 months is 0.36 ($p < 0.005$). The correlation in July and August is the most significant, with an r value of 0.48 and 0.49, respectively ($p < 0.001$) (only July is shown in Fig. 7b). This agrees well with the correlation between zonal wind and nssCa^{2+} .

Investigation of the influence of meridional wind on nssCa^{2+} concentration at IT001 shows no distinct correlation.

3.3. Relationships between IT015 nssCa^{2+} and atmospheric circulation, 1948–2001

NssCa^{2+} concentration in IT015 is close to that from IT001 and higher than that from SD (Table 2). The negative correlation between IT015 nssCa^{2+} concentration and zonal wind is significant ($p < 0.05$) at higher levels (700–300 hPa) in October and November. The best-correlated regions are the South Pacific and South America, and the southwest Indian Ocean (only November is shown in Fig. 8). Correlation investigations at different pressure levels indicate a more significant relationship when the atmospheric layer is higher. A negative correlation is also found between the nssCa^{2+} and AAO, and the most significantly correlated period is June–October (average $r = -0.27$, $p < 0.025$), especially October ($r = -0.38$, $p < 0.005$) when winds are strongest (Fig. 9). This negative correlation indicates that stronger westerly circulation does not favor transport of dust aerosols to IT015.

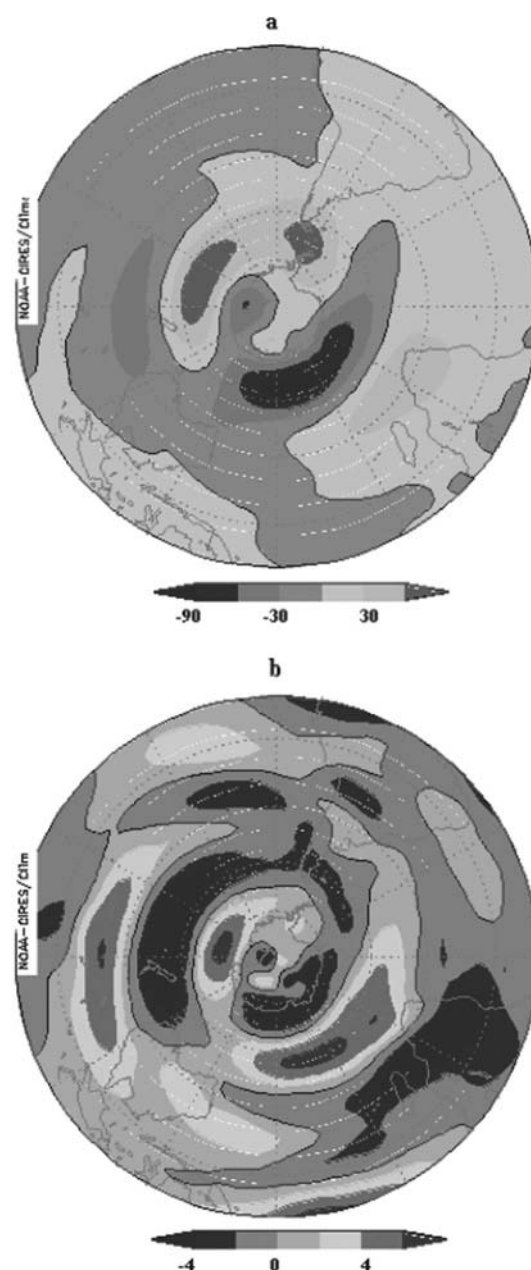


Fig. 4. Zonal anomalies (minus zonal mean) of seasonal mean geopotential height (a) and 500 hPa zonal wind (b) in the Southern Hemisphere during SON.

The reason for the negative correlation is unclear but may be related to high-latitude blocking on seasonal scales. This may impact IT015 differently from IT001 and SD because IT015 is significantly eastward of SD and IT001. Persistent, slow-moving anticyclones can interrupt regional weather sequences by 'blocking' the normal passage of cyclonic disturbances (Rex, 1950a,b; Trenberth and Mo, 1985). Studies by Van Loon (1956) and Lejenäs (1984) suggest that the highest frequency of SH blocking is in the New Zealand–southwest Pacific region, with secondary maxima east of South America and in the southwest Indian Ocean. Sinclair (1996) points out that anticyclones poleward of 50°S are related to an anomalous breakdown of the westerlies in regions southeast of Australia, New Zealand, South America and Africa that are especially prone to rapid anticyclone genesis. More persistent and intense blocking is largely confined to two regions in the South Pacific: southeast of

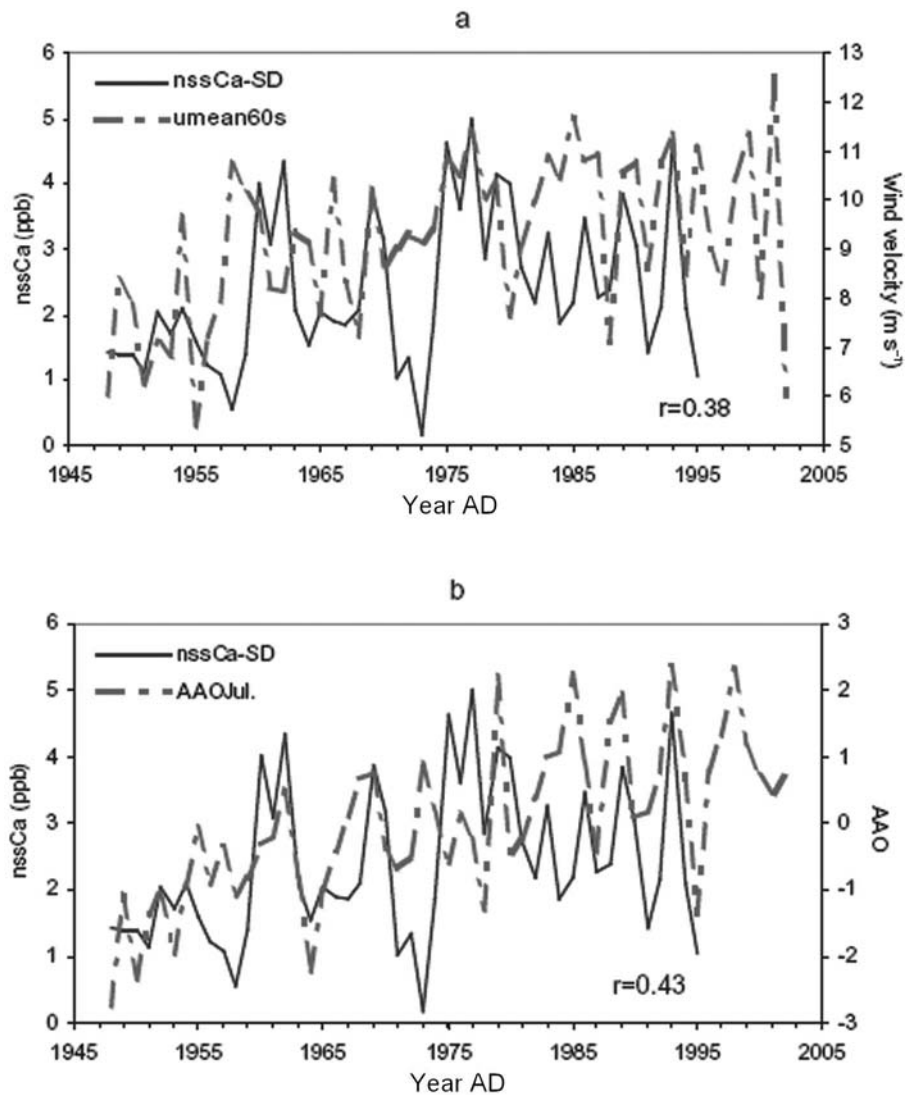


Fig. 5. Variation of SD nssCa^{2+} concentration and 850 hPa zonal mean wind at 60°S (a), and July AAO (b), for the period 1948–2002. r is the correlation coefficient.

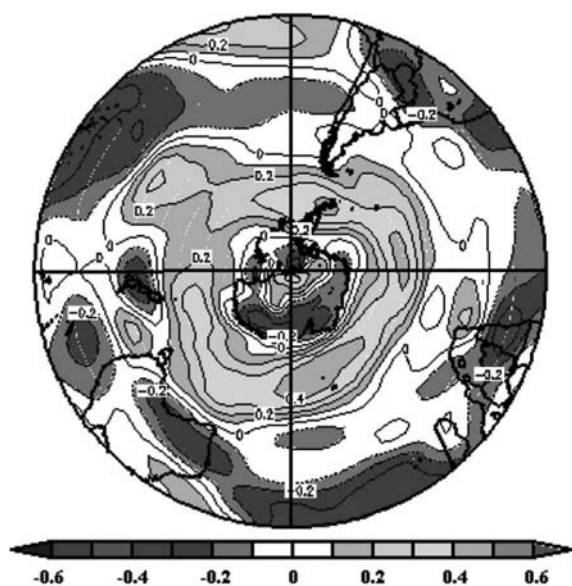


Fig. 6. Spatial correlation pattern of IT001 nssCa^{2+} concentration with 500 hPa zonal mean wind (only July is shown) for the period 1948–2002, plotted as correlation coefficients.

New Zealand and west of South America (Sinclair, 1996). Regions of significant negative correlation between IT015 nssCa^{2+} and atmospheric circulation are included in the blocking areas suggested by Van Loon (1956), Lejenäs (1984) and Sinclair (1996).

3.4. Connections between ENSO and nssCa^{2+}

Several studies have demonstrated a link between El Niño–Southern Oscillation (ENSO) and high-southern-latitude meteorology. Newell and others (1981) speculated that possible high-latitude forcing of the Southern Oscillation could be achieved by atmospheric forcing of the Antarctic circumpolar current. More recent research has focused on the role of South Pacific atmospheric double jet variability in the southward propagation of the ENSO signal (Smith and Bromwich, 1994; Smith and others, 1995; Chen and others, 1996). On the basis of its observed periodicity, White and Peterson (1996) speculate that initiation of the Antarctic Circumpolar Wave (ACW) is associated with ENSO activity in the equatorial Pacific, possibly through an atmospheric teleconnection with higher southern latitudes. Evidence of links to lower latitudes has been discovered through correlations between ENSO and moisture convergence in

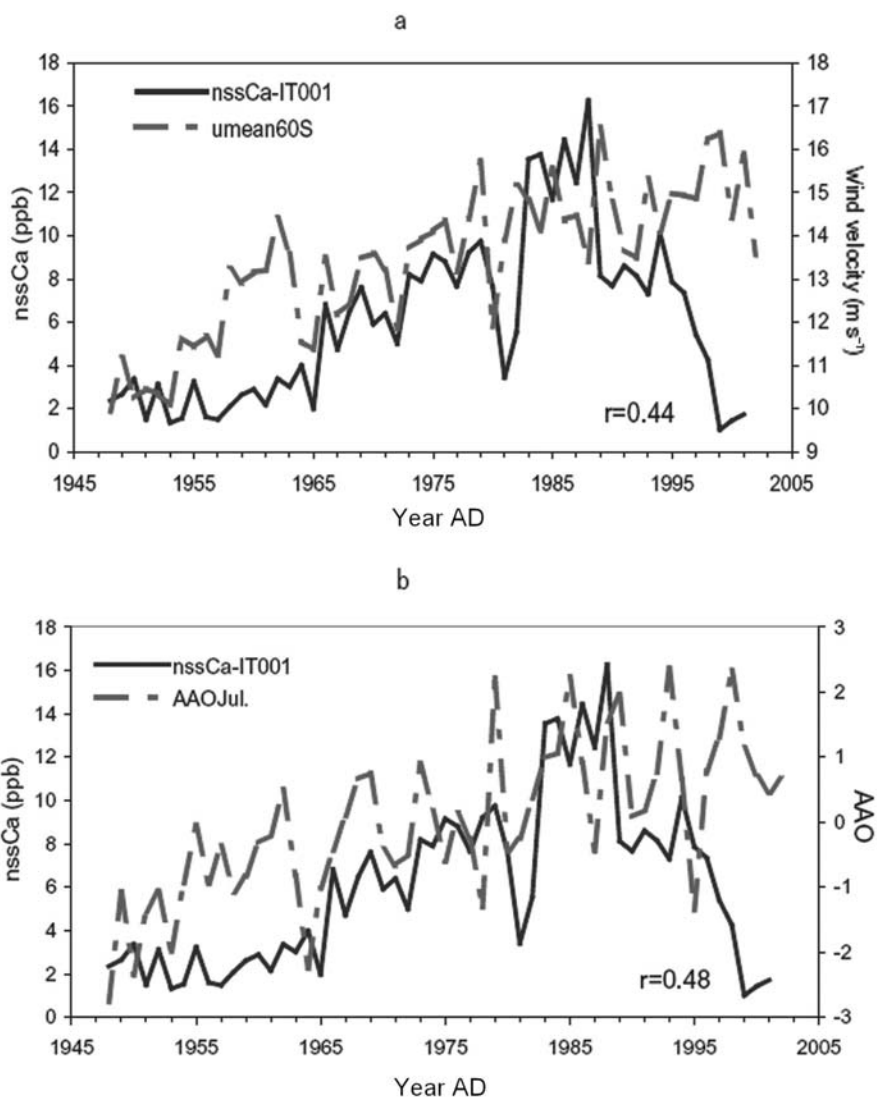


Fig. 7. Variation of IT001 nssCa²⁺ concentration and 500 hPa zonal mean wind at 60° S (a), and AAO (only July is shown) (b), for the period 1948–2002. *r* is the correlation coefficient.

a sector (75–90° S, 120–180° W) of West Antarctica (Cullather and others 1996). The nature of this teleconnection to tropical latitudes is unclear and its existence is still debated (Genthon and Krinner, 1998; Bromwich and others 2000). It may relate to changes in position and intensity of the Amundsen Sea low, as well as other changes in atmospheric circulation over the Antarctic Plateau as demonstrated by previous ice-core studies (Meyerson and others, 2002).

To find out if there are teleconnections between ENSO signals and crustal species concentrations in Antarctic snow, associations between the multivariate ENSO index (MEI; Wolter and Timlin, 1993, 1998) and nssCa²⁺ from the three ice cores were investigated. MEI integrates more information than other indices, reflecting the nature of the coupled ocean–atmosphere system better than either component, and is less vulnerable to occasional data glitches in the monthly update cycles (Wolter and Timlin, 1993, 1998).

The investigations show no correlation between MEI and nssCa²⁺ in SD and IT015. However, MEI is significantly correlated with nssCa²⁺ concentration in IT001 from January to March (average correlation coefficient is 0.32 (*p*<0.01)). The most significantly correlated period is

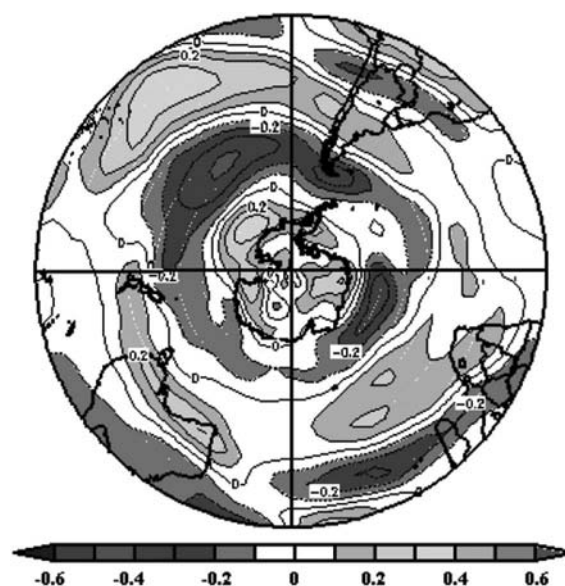


Fig. 8. Spatial correlation pattern of IT015 nssCa²⁺ concentration with 500 hPa zonal mean wind (only November is shown) for the period 1948–2001, plotted as correlation coefficients.

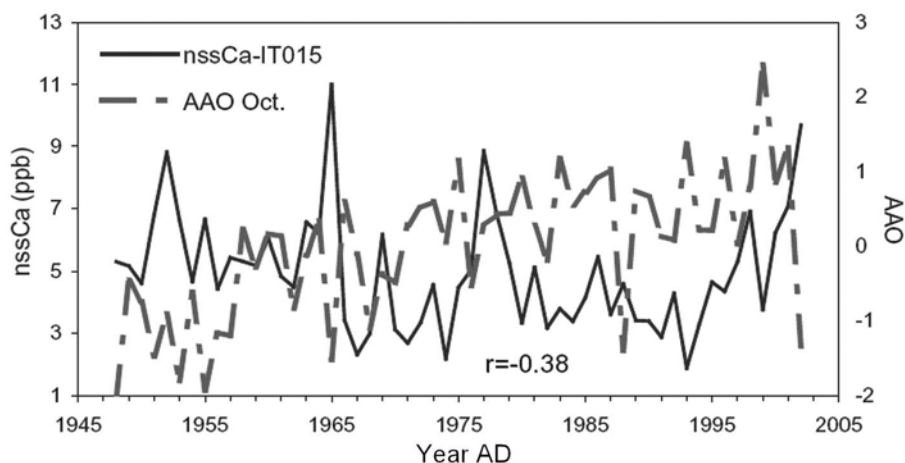


Fig. 9. Variation of IT015 nssCa^{2+} concentration and October AAO for the period 1948–2002. r is the correlation coefficient.

January–February (correlation coefficient 0.35, $p < 0.01$ ($p < 0.05$ also appears in April and May)). The MEI value for each month represents the average of 2 months (e.g. values in January represent the average over January and February). This suggests that crustal aerosols in IT001 are correlated with ENSO during the Southern Hemisphere summer. This possible link to the ENSO signal at the highest-elevation site (IT001) is consistent with our previous finding that crustal aerosols in the ice core come from the mid- to upper troposphere through vertical atmospheric movement. Figure 10 shows the correlation of nssCa^{2+} concentration in IT001 and MEI in January–February. During the strong ENSO period 1972–73 (Quinn and others, 1987; Legrand and Feniet-Saigne, 1991), nssCa^{2+} concentration increased by ~ 3 ppb, and the increase continued until 1979. The average nssCa^{2+} concentration during this period is about 8.7 ppb, 2.7 ppb higher than the 50 year mean value (Table 2). During the strongest ENSO event, in 1982–83, nssCa^{2+} concentration is the highest in the last 50 years. High concentrations continue until 1988 at ~ 14 ppb, 2.3 times the 50 year mean (the nssCa^{2+} concentration during this period is the highest in the last 350 years (not shown)). The concentrations stay high for several years and could be related to the propagating period of 4–5 years that ENSO may impart to the ACW (White and Peterson, 1996). Exceptionally, the strong ENSO event of 1957–58 is not recorded in IT001 nssCa^{2+} concentration.

One of the effects of El Niño events on global climate is that drought occurs in the western Pacific (southeastern Africa, India and the northeastern region of South America), an area normally rich in rainfall. During the most severe El Niño of the century, in 1982 and 1983, dust storms and brush fires ravaged eastern Australia as a result of decreased rainfall. Drought caused by the ENSO events in South Africa, Australia and South America resulted in land surface desertification and more dust aerosols in the atmosphere, especially in arid regions of those areas. The air mass containing these dust aerosols may have been transported to the high inland region of West Antarctica.

4. CONCLUSIONS

The relationships between atmospheric circulation and nssCa^{2+} concentrations from the three ice cores in West Antarctica are investigated using NCAR/NCEP data covering

the period 1948–2002. By performing spatial correlation analyses between the monthly NCAR/NCEP field and the nssCa^{2+} concentrations in the ice cores, we found that nssCa^{2+} concentration in SD is positively correlated with circumpolar zonal wind in SON. West-to-east pressure gradients intensified winds over the southeastern and southwestern Indian Ocean. Stronger westerly winds are conducive to the transport of crustal aerosols to SD. This is mostly connected to lower-layer circumpolar atmospheric circulation, such as the cyclonic systems around Antarctica that often move southward over the ice sheet. There is also a significant correlation between SD nssCa^{2+} concentrations and AAO from June to October over the last 50 years.

IT001 is mostly influenced by westerly circulation, resulting in higher nssCa^{2+} concentrations here than at the other two sites. The positive correlation between IT001 nssCa^{2+} concentration and the circumpolar higher-layer westerly wind exists throughout the year, indicating that IT001 is mainly influenced by the mid- to upper troposphere as expected due to its high elevation (Dixon and others, 2005). The regions most highly correlated to the zonal wind areas are South Africa, Australia and the southwestern Indian Ocean. IT001 nssCa^{2+} concentration is also correlated with AAO except in January, when westerly circulation is weakest and the wind is lightest.

The relationship of IT015 nssCa^{2+} concentration to atmospheric circulation is different to that of SD and IT001 nssCa^{2+} . The correlation of nssCa^{2+} with higher-layer zonal wind is significantly negative in October and November. The best-correlated regions are the South Pacific and South America, and the southwestern Indian Ocean. A negative correlation exists between IT015 nssCa^{2+} concentration and AAO, and the most correlated period of the AAO is October, when westerly winds are strongest. The negative correlation indicates that the stronger westerly circulation does not favor dust aerosol transport to IT015. The reason for the negative correlation is unclear but is probably related to high-latitude blocking on seasonal scales.

Correlations between meridional circulation and nssCa^{2+} concentrations from the three ice cores are not obvious, suggesting that the contribution of meridional circulation to crustal dust in SD, IT001 and IT015 is not significant. However, calibration between nssCa^{2+} concentration and MEI shows that more crustal species are transported to IT001 during the stronger ENSO event.

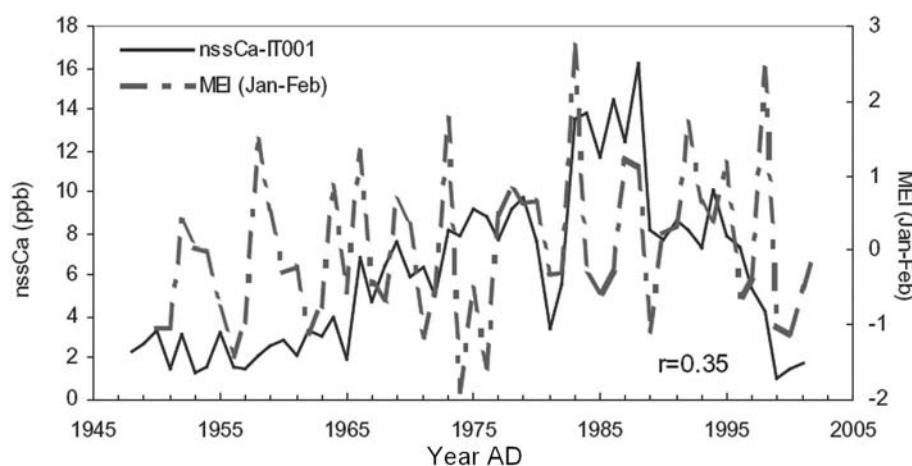


Fig. 10. Variation of IT001 nssCa^{2+} concentration and January–February MEI, 1948–2002. r is the correlation coefficient.

ACKNOWLEDGEMENTS

This research was supported by the US National Science Foundation Office of Polar Programs, the National Natural Science Foundation of China (40401054) and the 'Talent Project' of the Chinese Academy of Sciences. We greatly appreciate suggestions for the improvement of our paper from the referees and Scientific Editor, C Genthon.

REFERENCES

- Bromwich, D.H., F.M. Robasky, R.I. Cullather and M.L. van Woert. 1995. The atmospheric hydrologic cycle over the Southern Ocean and Antarctica from operational numerical analyses. *Mon. Weather Rev.*, **123**(12), 3518–3538.
- Bromwich, D.H., A.N. Rogers, P. Kållberg, R.I. Cullather, J.W.C. White and K.J. Kreutz. 2000. ECMWF analyses and reanalyses depiction of ENSO signal in Antarctic precipitation. *J. Climate*, **13**(8), 1406–1420.
- Budd, W.F., P.A. Reid and L.J. Minty. 1995. Antarctic moisture flux and net accumulation from global atmospheric analyses. *Ann. Glaciol.*, **21**, 149–156.
- Carleton, A.M. 1989. Antarctic sea-ice relationships with indices of the atmospheric circulation of the Southern Hemisphere. *Climate Dyn.*, **3**(4), 207–220.
- Chen, B., S.R. Smith and D.H. Bromwich. 1996. Evolution of the tropospheric split jet over the South Pacific Ocean during the 1986–1989 ENSO cycle. *Mon. Weather Rev.*, **124**(8), 1711–1731.
- Cullather, R.I., D.H. Bromwich and M.L. van Woert. 1996. Interannual variations in Antarctic precipitation related to El-Niño–Southern Oscillation. *J. Geophys. Res.*, **101**(D14), 19,109–19,118.
- Cullather, R.I., D.H. Bromwich and R.W. Grumbine. 1997. Validation of operational numerical analyses in Antarctic latitudes. *J. Geophys. Res.*, **102**(D12), 13,761–13,784.
- Davidson, C.I., J.L. Jaffrezo and P.A. Mayewski. 1992. Arctic air pollution as reflected in snowpits and ice cores. In Sturges, W.T., ed. *Pollution of the Arctic atmosphere*. New York, Elsevier, 43–95.
- Delmas, R.J. and M. Legrand. 1989. Long-term changes in the concentrations of major chemical compounds (soluble and insoluble) along deep ice cores. In Oeschger, H. and C.C. Langway, Jr, eds. *The environmental record in glaciers and ice sheets*. Chichester, etc., John Wiley and Sons, 319–341.
- Dixon, D. and 7 others. 2005. 200 year sulfate record from Antarctic ice cores. *Ann. Glaciol.*, **41** (see paper in this volume).
- Fischer, H. 2001. Imprint of large-scale atmospheric transport patterns on sea-salt records in northern Greenland ice cores. *J. Geophys. Res.*, **106**(D20), 23,977–23,984.
- Genthon, C. and G. Krinner. 1998. Convergence and disposal of energy and moisture on the Antarctic polar cap from ECMWF analyses and forecasts. *J. Climate*, **11**(7), 1703–1716.
- Harris, J.M. 1992. An analysis of 5-day midtropospheric flow patterns for the South Pole. *Tellus*, **44B**, 409–421.
- Herron, M.M. 1982. Impurity sources of F^- , Cl^- , NO_3^- and SO_4^{2-} in Greenland and Antarctic precipitation. *J. Geophys. Res.*, **87**(C4), 3052–3060.
- Kalnay, E. and 21 others. 1996. The NCEP/NCAR 40-year reanalysis project. *Bull. Am. Meteorol. Soc.*, **77**(3), 437–471.
- Kang, S. and 7 others. 2002. Glaciochemical records from a Mt. Everest ice core: relationship to atmospheric circulation over Asia. *Atmos. Environ.*, **36**, 3351–3361.
- Kang, S., P.A. Mayewski, Y. Yan and D. Qin. 2003. Dust records from three ice cores: relationships to spring atmospheric circulation over the Northern Hemisphere. *Atmos. Environ.*, **37**(34), 4823–4835.
- Kaspari, S. and 6 others. 2004. Climate variability in West Antarctica derived from annual accumulation rate records from ITASE firn/ice cores. *Ann. Glaciol.*, **39**, 585–594.
- Kreutz, K.J. and P.A. Mayewski, 1999. Survey of Antarctic surface snow glaciochemistry. *Antarct. Sci.*, **11**(1), 105–118.
- Kreutz, K.J., P.A. Mayewski, M.S. Twickler and S.I. Whitlow. 1996. Glaciochemical reconnaissance in inland West Antarctica. *Antarct. J. US*, **31**(2), 51–52.
- Kreutz, K.J., P.A. Mayewski, L.D. Meeker, M.S. Twickler, S.I. Whitlow and I.I. Pittalwala. 1997. Bipolar changes in atmospheric circulation during the Little Ice Age. *Science*, **277**(5330), 1294–1296.
- Kreutz, K.J. and 11 others. 1999. Seasonal variations of glaciochemical, isotopic and stratigraphic properties in Siple Dome (Antarctica) surface snow. *Ann. Glaciol.*, **29**, 38–44.
- Kreutz, K.J., P.A. Mayewski, I.I. Pittalwala, L.D. Meeker, M.S. Twickler and S.I. Whitlow. 2000. Sea level pressure variability in the Amundsen Sea region inferred from a West Antarctic glaciochemical record. *J. Geophys. Res.*, **105**(D3), 4047–4059.
- Legrand, M. and C. Feniet-Saigne. 1991. Methanesulfonic acid in south polar snow layers: a record of strong El Niño? *Geophys. Res. Lett.*, **18**(2), 187–190.
- Legrand, M. and P. Mayewski. 1997. Glaciochemistry of polar ice cores: a review. *Rev. Geophys.*, **35**(3), 219–243.
- Lejenäs, H. 1984. Characteristics of Southern Hemisphere blocking as determined from a time series of observation data. *QJR Meteorol. Soc.*, **110**, 967–979.
- Lyons, W.B. and P.A. Mayewski. 1984. Glaciochemical investigations as a tool in the historical delineation of the acid precipitation problem. In Althuller, A.P. and R.P. Linthurst, eds. *The acidic deposition phenomenon and its effects*. Raleigh, NC, 8-71–8-81.

- Mayewski, P.A. and W.B. Lyons. 1982. Source and climatic implication of the reactive iron and reactive silicate concentrations found in a core from Meserve Glacier, Antarctica. *Geophys. Res. Lett.*, **9**(3), 190–192.
- Mayewski, P.A., M.J. Spencer and W.B. Lyons. 1992. A review of glaciochemistry with particular emphasis on the recent record of sulfate and nitrate. In Moore, B. and S. David, eds. *Proceedings of the 1988 OIED Global Change Institute: Trace Gases and the Biosphere*. Boulder, CO, University Corporation for Atmospheric Research/Office of Interdisciplinary Earth Studies, 177–199.
- Mayewski, P.A. and 8 others. 1993. Greenland ice core “signal” characteristics: an expanded view of climate change. *J. Geophys. Res.*, **98**(D7), 12,839–12,847.
- Mayewski, P.A., M.S. Twickler and S.I. Whitlow. 1995. The Siple Dome ice core: reconnaissance glaciochemistry. *Antarct. J. US*, **30**(5), 85–87.
- Mayewski, P.A. and 6 others. 1997. Major features and forcing of high-latitude Northern Hemisphere atmospheric circulation using a 110,000-year-long glaciochemical series. *J. Geophys. Res.*, **102**(C12), 26,345–26,366.
- Meeker, L.D. and P.A. Mayewski. 2002. A 1400-year long record of atmospheric circulation over the North Atlantic and Asia. *The Holocene*, **12**(3), 257–266.
- Meyerson, E.A., P.A. Mayewski, K.J. Kreutz, L.D. Meeker, S.I. Whitlow and M.S. Twickler. 2002. The polar expression of ENSO and sea-ice variability as recorded in a South Pole ice core. *Ann. Glaciol.*, **35**, 430–436.
- Mumford, J.W. and D.A. Peel. 1982. Microparticles, marine salts and stable isotopes in a shallow firn core from the Antarctic Peninsula. *Brit. Antarct. Surv. Bull.*, **56**, 37–47.
- Newell, R.E., L.S. Chiu, W. Ebisuzaki, A.R. Navato and H.B. Selkirk. 1981. The oceans and ocean currents: their influence on climate. In *International Conference on Climate and Offshore Energy Resources*. Boston, MA, American Meteorological Society, 59–112.
- O'Brien, S.R., P.A. Mayewski, L.D. Meeker, D.A. Meese, M.S. Twickler and S.I. Whitlow. 1995. Complexity of Holocene climate as reconstructed from a Greenland ice core. *Science*, **270**(5244), 1962–1964.
- Quinn, W.H., V.T. Neal and S.E. Antunez de Mayolo. 1987. El Niño occurrences over the past four and a half centuries. *J. Geophys. Res.*, **92**(C13), 14,449–14,461.
- Reijmer, C.H., M.R. van den Broeke and M.P. Scheele. 2002. Air parcel trajectories and snowfall related to five deep drilling locations on Antarctica based on the ERA-15 dataset. *J. Climate*, **15**(14), 1957–1968.
- Rex, D.F. 1950a. Blocking action in the middle troposphere and its effects upon regional climate. I: An aerological study of blocking action. *Tellus*, **2**, 196–211.
- Rex, D.F. 1950b. Blocking action in the middle troposphere and its effect upon regional climate. II: The climatology of blocking action. *Tellus*, **2**, 275–301.
- Rogers, J.C. 1983. Spatial variability of Antarctic temperature anomalies and their association with the Southern Hemisphere atmospheric circulation. *Ann. Assoc. Amer. Geog.*, **73**(4), 502–518.
- Röthlisberger, R. and 6 others. 2002. Dust and sea salt variability in central East Antarctica (Dome C) over the last 45 kyrs and its implications for southern high-latitude climate. *Geophys. Res. Lett.*, **29**(20), 1963. (10.1029/2002GL015186.)
- Shaw, G.E. 1989. Aerosol transport from sources to ice sheets. In Oeschger, H. and C.C. Langway, Jr, eds. *The environmental record in glaciers and ice sheets*. Chichester, etc., John Wiley and Sons, 13–27.
- Simmonds, I. and K. Keay. 2000. Mean Southern Hemisphere extratropical cyclone behaviour in the 40-year NCEP–NCAR reanalysis. *J. Climate*, **13**, 873–885.
- Sinclair, M.R. 1996. Climatology of anticyclones and blocking for the Southern Hemisphere. *Mon. Weather Rev.*, **124**, 245–263.
- Smith, S.R. and D.H. Bromwich. 1994. Behavior of the tropospheric split jet stream over the South Pacific Ocean during 1986–1990 ENSO cycle. In *Proceedings of the Sixth Conference on Climate Variations, American Meteorological Society, Nashville, TN, January 23–28, 1994*. Boston, MA, American Meteorological Society, 278–282.
- Smith, S.R., D.H. Bromwich and B. Chen. 1995. Split jet evolution over the South Pacific Ocean during the 1986–1989 ENSO cycle. In *Proceedings of the Fourth Conference on Polar Meteorology and Oceanography, American Meteorological Society, Dallas, TX, January 10–15, 1995*. Boston, MA, American Meteorological Society, 246–251.
- Sommer, S. and 9 others. 2000. Glacio-chemical study spanning the past 2 kyr on three ice cores from Dronning Maud Land, Antarctica. 1. Annually resolved accumulation rates. *J. Geophys. Res.*, **105**(D24), 29,411–29,421.
- Souney, J., P.A. Mayewski, I. Goodwin, V. Morgan and T. van Ommen. 2002. A late Holocene climate record from Law Dome, East Antarctica. *J. Geophys. Res.*, **107**(D22), 4608–4617.
- Steffensen, J.P. 1988. Analysis of the seasonal variation in dust, Cl^- , NO_3^- , and SO_4^{2-} in two central Greenland firn cores. *Ann. Glaciol.*, **10**, 171–177.
- Thompson, D.W.J. and J.M. Wallace. 2000. Annular modes in the extratropical circulation. Part I: Month-to-month variability. *J. Climate*, **13**(5), 1000–1016.
- Trenberth, K.E. 1992. *Global analyses from ECMWF and atlas of 1000 to 10 mb circulation statistics*. Boulder, CO, National Center for Atmospheric Research.
- Trenberth, K.E. 1995. Atmospheric circulation climate changes. *Climatic Change*, **31**(2–4), 427–453.
- Trenberth, K.E. and K.C. Mo. 1985. Blocking in the Southern Hemisphere. *Mon. Weather Rev.*, **113**, 3–21.
- Trenberth, K.E. and A. Solomon. 1994. Implications of global atmospheric spatial spectra for processing and displaying data. *J. Climate*, **6**, 531–545.
- Van Loon, H. 1956. Blocking action in the Southern Hemisphere, Part I. *Notos*, **5**, 171–178.
- Wagenbach, D. 1996. Coastal Antarctica: atmospheric chemical composition and atmospheric transport. In Wolff, E.W. and R.C. Bales, eds. *Chemical exchange between the atmosphere and polar snow*. New York: North Atlantic Treaty Organization. (NATO ASI Series 43.)
- White, W.B. and R.G. Peterson. 1996. An Antarctic circumpolar wave in surface pressure, wind, temperature and sea-ice extent. *Nature*, **380**(6576), 699–702.
- Whitlow, S.I., P.A. Mayewski and G. Holdsworth. 1994. An ice core based record of biomass burning in North America, 1750–1980. *Tellus*, **380B**, 699–702.
- Wolff, E.W., A.M. Rankin and R. Röthlisberger. 2003. An ice core indicator of Antarctic sea ice production? *Geophys. Res. Lett.*, **30**(22), 2158. (10.1029/2003GL018454.)
- Wolter, K. and M.S. Timlin. 1993. Monitoring ENSO in COADS with a seasonally adjusted principal component index. In *Proceedings of the 17th Climate Diagnostics Workshop*. Norman, OK, National Oceanic and Atmospheric Administration Climate Analysis Center, National Severe Storms Laboratory, Center for Integrative Multiscale Modeling and Simulation and the School of Meteorology, University of Oklahoma, 52–57.
- Wolter, K. and M.S. Timlin. 1998. Measuring the strength of ENSO events: how does 1997/98 rank? *Weather*, **53**, 315–324.